FLIGHT CONTROL LAWS FOR THE QUADCRUISER RPA

M. Hanel, M. Haimerl, T. Bienert, Airbus Defence & Space, Manching, Germany

Abstract

This paper describes the flight control functionality for the Quadcruiser remotely piloted air vehicle (RPA). The Quadcruiser is a hybrid air vehicle featuring both an electrically powered lift system for a vertical take-off, landing and hover capability and a combustion engine powered cruise flight capability with wing, empennage and conventional control surfaces. For transition between hover and cruise both the lift system and the cruise control system are active. The flight control functionality features stability augmentation and attitude control for hover, cruise and transition and flight guidance functionality for altitude, speed and direction control. The functionality has been implemented and flight-test-demonstrated on a fully electric sub-scale experimental vehicle, the QC11.

1. INTRODUCTION

The Quadcruiser project of Airbus Defence and Space studies the concept of a remotely piloted hybrid air vehicle with a take-off mass of approx. 500kg (see FIG 1) and a wing span of 9m featuring

- an electric lift system for vertical take-off and landing and hover flight; and
- wing, empennage and a combustion engine for cruise flight.

When active, the electric lift system would be powered both from batteries and the combustion engine power train. The batteries would be re-charged from the latter during cruise flight, providing energy for hover sequences as part of the vehicle missions.

The project aims at innovation and technology demonstration in the areas of hybrid propulsion and safe flight of remotely piloted air vehicles and is conducted in cooperation with research partners from industry and academia.

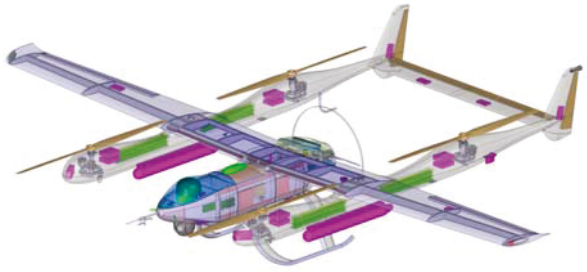

FIG 1. Quadcruiser hybrid air vehicle

With respect to airworthiness, the design target for the Quadcruiser is civil certification for flight over populated areas, resulting in tough requirements on system reliability and failure tolerance. The system design addresses these requirements e.g. by redundancies which in the area of flight control is reflected in the number of contol devices installed:

- four sets of counter-rotating lift propellers driven by eight electric motors;
- two ailerons, elevators and rudders;
- a combustion engine driving the push propeller with blade pitch control and a clutch for disengagement.

As the quadcruiser air vehicle configuration is unconventional with respect to hover flight and to transition between hover and cruise, it was decided to build a subscale experimental vehicle - the QC11 (see FIG 2) - for studying the flight dynamics of the air vehicle and suitable flight control strategies for hover and transition as part of the concept studies for the target vehicle. This subscale demonstrators follows earlier studies of a 10kg proof-of-concept demonstrator, the QC10 (see e.g. [2]).

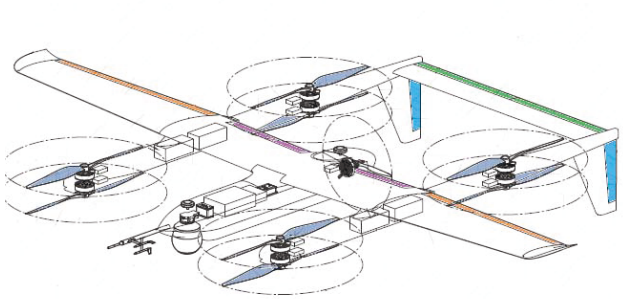

FIG 2. Quadcruiser QC11 subscale demonstrator

QC11 is fully electric and has a take-off mass of 35kg, see TAB 1. Push propeller blade pitch control and clutch are replaced by rotation control of the electric motor. Two flaps are installed on the trailing edge of the inner wing for studying the benefit of high lift devices during transition.

MTOM	35kg	Ref. Area	$1.2m^2$
Wing Span	3,5m	l_μ, MAC	0,36m
Lift Prop	30 x 10,5	Lift Motor	T-mot U10+
Push Prop	22 x 18	Push Motor	Hacker Q80

TAB 1. Quadcruiser subscale air vehicle characteristics

doi:10.25967/480033

This paper is based on the results of the flight dynamics investigation, the control law prototype design and the flight test of QC11. It is expected that these results are representative (after appropriate scaling) for the target size of Quadcruiser. This is supported by the results of aerodynamic investigations on the target size Quadcruiser based on CFD calculations and propeller rig tests.

2. BASIC FLIGHT MECHANICS OF THE QUADCRUISER VEHICLE IN HOVER AND CRUISE

Interference effects between the eight lift propellers, wing and empennage of the Quadcruiser [3] have a strong impact on the stability characteristics of the vehicle in hover flight with pitch and yaw axis stability changing from stable in headwind conditions to unstable in tailwind conditions, see TAB 2. The roll axis is only unstable in crosswind conditions but neutrally stable under both head- and tailwind conditions. The Quadcruiser exhibits a pitch up moment in headwind conditions and a pitch down moment in tailwind conditions. The roll moment in sidewind conditions behaves accordingly. Drag appears in wind conditions from every direction, with higher drag values found in sidewind and tailwind conditions.

u [m/s]	10	-10
time to double pitch axis [s]	0,9	0,3
time to double yaw axis [s]	stable	2,3

TAB 2. QC11 flight mechanic characteristics in hover

In cruise flight, the empennage ensures open-loop stable pitch, roll and yaw axes dynamics, see TAB 3.

V [kts]	40 (V_{Stall})	80 (V_{max})
AoA@1g-trim@35kg [deg]	9	-1.2
short period freq/damp [rad/s;-]	4.2 / 0.56	7 / 0.7
roll mode frequency [rad/s]	3.7	7.7
dutch roll freq./damp [rad/s;-]	2.1 / 0.18	3.7 / 0.15

TAB 3. QC11 flight mechanic characteristics in cruise

As the transition between hover and cruise flight had been seen as the biggest control challenge for Quadcruiser, a comparatively high longitudinal stability of 35% l_m has been chosen for the pitch axis of the subscale demonstrator. This would simplify pitch axis control in case the transition was performed by simply switching off the lift motors at small forward speed and waiting for the aircraft to speed up due to altitude loss and propulsion from the cruise motor/propeller combination.

It was later found that for the subscale demonstrator the transition can be performed with lift and cruise motors running at the same time and up to the stall speed of the vehicle without causing excessive vibrations so that the transition can be performed at almost constant altitude.

The Quadcruiser flight envelope (see FIG 3) is split into three segments, for hover, transition and cruise respectively. In hover flight, only the lift system is active, in cruise flight only the pusher and the aerodynamic control surfaces are active whereas in transition (or “copter” mode) all control effectors are used.

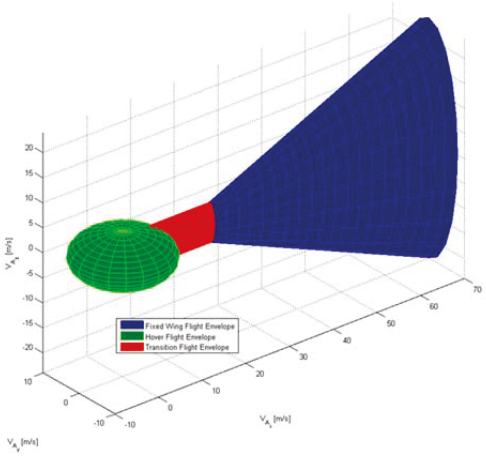

FIG 3. Speed Envelope for Hover, Transition and Cruise

The forward/backward speed boundaries in Hover flight are denoted $V_{maxHover}$, $V_{minHover}$ respectively whereas the min/max speed boundaries in cruise flight are denoted V_{minFCS} (12) and V_{max} respectively.

3. CONTROL LAWS FOR HOVER AND CRUISE

3.1. Control Laws for Hover

In hover, changes to the rotation of motion of the 8 lift propellers are the control devices for generating lift (T_{cmd}) and roll (L_{cmd}), pitch (M_{cmd}) and yaw (N_{cmd}) moments used for direct control of the vehicles’ three rotational degrees of freedom and the vertical translational degree of freedom. The remaining two translational degrees of freedom can be controlled by tilting of the lift vector.

3.1.1. Control Law Bandwidth Hover

The achievable control law bandwidth in hover depends on the open loop dynamics of the plant. The required control bandwidth depends on the stability characteristics and the acceptable control error, e.g. the position deviation during landing caused by wind disturbances. The time response characteristics of the hover control system consisting of eight lift motors with propellers can be approximated by a first order lag filter with a time constant of 70ms. The worst case time lag of IMU, FCC and Bus is 35ms.

Cross over frequency [rad/s]	
Pitch Attitude Control	5,0
Roll Attitude Control	5,0
Yaw Rate Control	2,0
Height Rate Control	2,5

TAB 4. Control Law Bandwidth Hover

In order to avoid feedback/propagation of vibrations and excitation of structural eigenfrequencies, anti-aliasing, notch and roll-off filters are implemented.

The control law bandwidth achieved for the hover flight control loops is shown in TAB 4.

3.1.2. Control Allocation

A dedicated control allocation is set up to map the roll, pitch, yaw moment and the collective lift demand to single engine inputs, see FIG 4. It ensures decoupling of the mentioned control moments/forces.

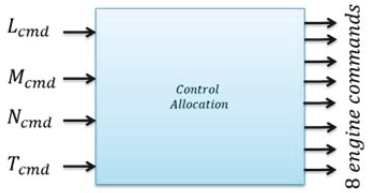

FIG 4. Control Allocation in Hover

3.1.3. Attitude Control

Pitch Axis damping is increased by proportional feedback of pitch rate on pitch moment demand. Stabilization is provided by a proportional-integral feedback of pitch attitude. Integral feedback ensures trim of the vehicle. The Roll Axis is controlled in the same way.

Additional phase advance filtering of roll and pitch rate is required to at least partly compensate the lag of signal filtering, sensors and engines with the aim of ensuring the required bandwidth for overcoming the instability in these axes. FIG 5 shows the attitude control in the pitch axis (roll axis equivalent).

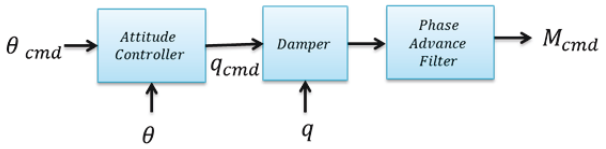

FIG 5. Attitude Control in the pitch axis

Yaw axis damping is increased by proportional feedback of yaw rate on yaw moment demand and integral feedback of yaw rate ensures trim and steady state accuracy, see FIG 6. A phase advance filter is not required in the yaw axis due to the lower required bandwidth.

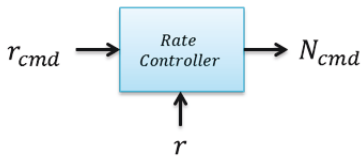

FIG 6. Rate Control in yaw axis

3.1.4. Velocity Control

Velocity control in longitudinal direction is performed by tilting of the collective lift vector via pitch attitude command, see FIG 7.

Proportional-Integral feedback of longitudinal velocity ensures damping of position control and trim to overcome drag. Absolute limitation on pitch attitude command avoids critical vehicle orientations. The lateral axis is controlled in the same way.

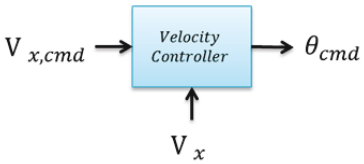

FIG 7. Velocity Control in longitudinal direction

The vertical axis is controlled by increasing and decreasing collective lift. Proportional-Integral feedback of climb rate increases damping and ensures zero steady state error in the vertical axis, see FIG 8.

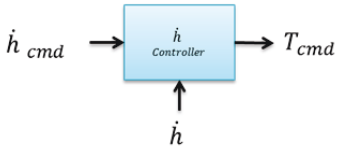

FIG 8. Height Rate Control

3.1.5. Position Control

Position control is provided by proportional feedback of position deviation in longitudinal, lateral and vertical axis, see FIG 9 for example in longitudinal direction (lateral and vertical axis accordingly). Limitations on commanded velocities ensure envelope protection.

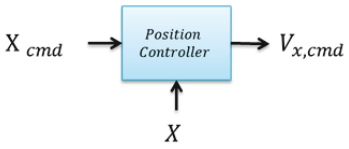

FIG 9. Position Control in longitudinal direction

3.2. Implementation of Hover Flight Control and Flight Test Results

A cascaded feedback system is used for hover flight control laws. Most inner loops combine rate feedback with moment/force demand based on rate error.

(1)
$$L_{cmd} = k_p \cdot (p_{cmd} - p)$$
$$M_{cmd} = k_q \cdot (q_{cmd} - q)$$
$$N_{cmd} = k_r \left(1 + k_{ri} \frac{1}{s}\right) \cdot (r_{cmd} - r)$$
$$T_{cmd} = k_{\dot{h}} \left(1 + k_{\dot{h}i} \frac{1}{s}\right) \cdot (\dot{h}_{cmd} - \dot{h})$$

where $k_p, k_q, k_r, k_{\dot{h}}$ are the proportional and $k_{ri}, k_{\dot{h}i}$ are the integral feedback gains. Moment demand is phase advance filtered in pitch and roll axis to compensate for hover engines and IMU/FCS delay. This is needed to achieve high bandwidth in roll and pitch axis to overcome instabilities in these axes. The following 2nd order transfer function is applied for phase advance filtering:

(2)
$$G(s) = \frac{0{,}006s^2 + 0{,}1231s + 1}{0{,}0014s^2 + 0{,}0593s + 1}$$

A rate and absolute limit is applied to all moment/force demands. Control allocation distributes moment/force demands to engine demands.

Proportional and integral gains in the yaw axis are chosen for adequate damping/stabilization in tailwind conditions

and for shaping the yaw rate command response. Due to slow yaw axis dynamics, see TAB 2, stabilization can be performed without phase advance filter on the yaw moment demand.

The altitude rate feedback loop needs a high bandwidth to overcome the coupling between pitch attitude and heave motion found at airspeeds exceeding approx. 5m/s as both motions change angle-of-attack (and consequently lift on the wing). Since no measurement of airflow conditions in hover is available, a cross compensation is not implemented.

The next outer cascade for pitch and roll axis consists of attitude control: It is based on attitude proportional and integral feedback on rate command, see eq. (3) for pitch attitude control (roll attitude control similar).

(3) $$q_{cmd} = k_\theta \left(1 + k_{\theta i}\frac{1}{s}\right) \cdot (\theta_{cmd} - \theta)$$

where k_θ denotes the proportional and $k_{\theta i}$ the integral feedback gain. The gains are chosen such that the relative damping is greater than 0,7.

Velocity control in the longitudinal and lateral axes consists of proportional-integral feedback of velocity error on attitude command (vy control similar):

(4) $$\theta_{cmd} = k_{vx} \left(1 + k_{vxi}\frac{1}{s}\right) \cdot (v_{x,cmd} - v_x)$$

where k_{vx} is the proportional and k_{vxi} the integral feedback gain. Attitude command corresponds to a tilting of collective lift vector in the desired direction. This force from collective lift is used to overcome drag and for accelerating in the desired direction.

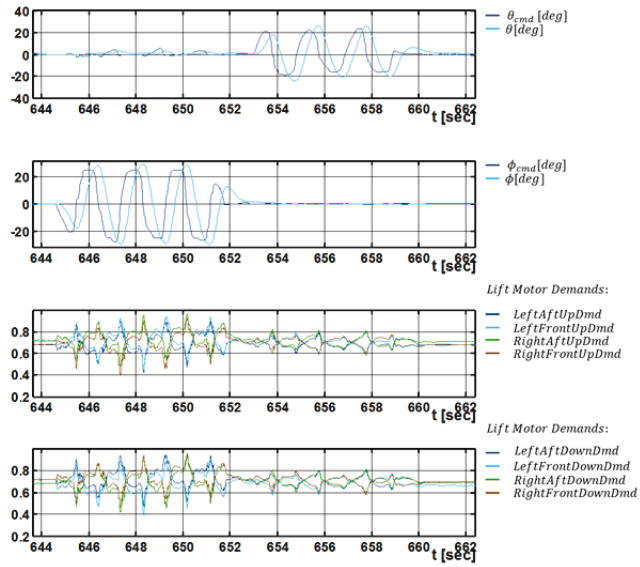

FIG 10. Hover Flight Test – Attitude manoeuvres

Position and height control is performed with proportional feedback of position/height error on velocity/height rate command, see eq. (5) for example in X-direction.

(5) $$v_{x,cmd} = k_x \cdot (X_{cmd} - X)$$

where k_x is the proportional feedback gain.

The implementation of the control algorithm uses the differential PI algorithm [1]. The integrators are moved downstream of the control allocation, representing the states of the 8 lift engines. Proportional feedback is implemented with derivation of signals and integral feedback with proportional feedback of signals. Additional slow feedback loops are introduced to bind four of the eight integrators, which are not used for trim of the vehicle.

3.2.1. Hover Flight Test Results

Hover Flight Testing was split in two parts. The first part concentrated on attitude control with a Remote Pilot controlling velocity and position of the Quadcruiser. Different inputs were given by the pilot to test the vehicle's closed loop behaviour such as a bank to bank or a pitch sweep manoeuvre. FIG 10 shows a corresponding flight test. The vehicle is able to follow the attitude commands properly and all lift motor demands stay in an acceptable range. Additional full climb, dive and yaw rate inputs have been flight tested to assess the vehicles flying qualities.

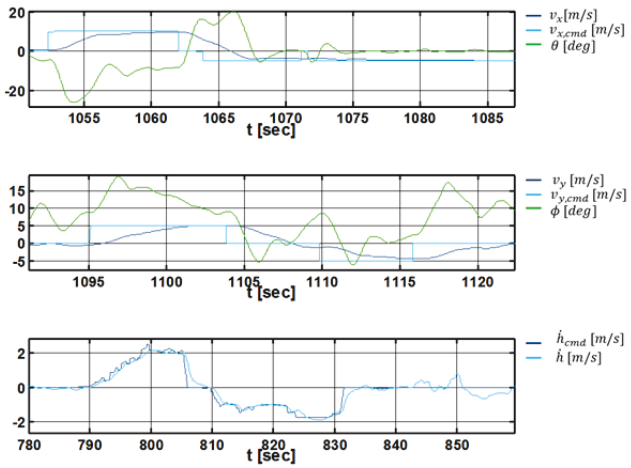

FIG 11. Hover Flight Test – Velocity manoeuvres

The second part focused on the test of the outer control loops, which contain the velocity and the position control.

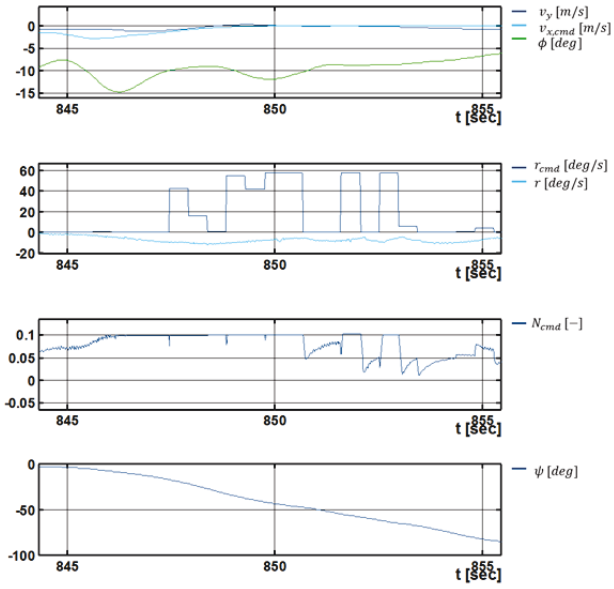

FIG 12. Hover Flight Test – Yaw Moment Limitation

Therefore, different velocities have been commanded to the vehicle. FIG 11 compares the different commanded velocities with the achieved velocities in flight test. As it can be seen in this figure, the vehicle follows the

commanded velocities as designed, however a high variation of attitude angles is needed to compensate for wind/disturbances.

One of the main characteristics of the QC11 compared to other multicopters in hover flight is it's weather cock stability. FIG 12 illustrates a flight test where the vehicle is flying in steady state side wind conditions.

The yaw moment created by the airflow at the vertical tail has to be compensated by the hover engines. As the yaw moment limit in the control laws is reached at time 846, the vehicle starts to yaw into the wind. The steady state bank angle of about 10° which is needed to maintain zero lateral velocity is a measure of the sidewind strength (see eq. (11) below).

3.3. Control Laws for Cruise

In cruise flight, left and right sets of ailerons, elevators and rudders are available for creating roll, pitch and yaw moments respectively and the push propeller speed (QC11 only) is varied for thrust control. The control laws are implemented using the differential PI algorithm (see e.g. [1], chapter 19) with integrator outputs representing the aileron, elevator, rudder and PLA commands respectively.

3.3.1. Stability Augmentation

Judging from the Quadcruiser QC11's open-loop stability properties (see TAB 3), it is concluded that a yaw damper for dutch roll damping increase to a damping coefficient of at least 0.35 is desired whereas stability augmentation for short period mode and roll mode is more of an opportunity for flying qualities optimisation.

The end-to-end delay from IMU-excitation to servo deflection has been determined by turn-table tests in the frequency range up to 5Hz, with a value of 75ms (equivalent to 135deg phase loss at 5Hz) obtained as a result. Consequently the available control law bandwidth is considered largely sufficient for stability augmentation of short period, roll and dutch roll mode.

3.3.2. Attitude Control

Integral load factor control is implemented in the pitch axis with a pitch damper ($k_q q$) for short-period mode damping augmentation and complemented by a small stiffness feedback ($k_{\hat{\alpha}}\hat{\alpha}$, using a pitch-rate-derived angle-of-attack estimate) for compensating the destabilising effect of the integral load factor feedback, eq. (6).

$$\eta_{cmd} = -k_q q - k_{\hat{\alpha}}\hat{\alpha} + \frac{k_{i,nz}}{s}(nz_{cmd} - nz) \quad (6)$$

Angle-of-attack protection is provided based on measured angle-of-attack, replacing integral load factor by integral angle-of-attack feedback in case the angle-of-attack limit is violated.

In the lateral axes, a proportional-integral bank angle control system is implemented. A roll damper is added for roll mode augmentation and a yaw damper for dutch-roll mode damping augmentation, eq. (7).

$$\begin{aligned} \xi_{cmd} &= -k_p p - k_{x,r} r + \left(k_\phi + \frac{k_{i,\phi}}{s}\right)(\phi_{cmd} - \phi) \\ \zeta_{cmd} &= -k_{z,p} p - k_r r + \left(\frac{k_{i,\beta}}{s}\right)\dot{\beta}_{est} \\ \dot{\beta}_{est} &= \frac{g}{V} sin(\phi) - r \end{aligned} \quad (7)$$

Turn coordination is ensured by integral feedback of a sideslip rate estimate $\dot{\beta}_{est}$ derived from yaw rate and bank angle measurements.

The control surfaces are sized such that a single control surface in each axis is sufficient to control the vehicle for safe flight (albeit at reduced performance) if the other control surface is at zero position or free floating. For the target design of a certifiable Quadcruiser this is complemented by actuators featuring a clutch on the connection to the control surface so that the control surface is free floating when the clutch is released. Consequently, the control strategy in case of single actuator or control surface failure is to bring the failed surface to zero or free-floating and re-configure the control laws accordingly. For the subscale technology demonstrator simple servos are used, so that failure detection and control law re-configuration is not possible. It is planned however to prototype the re-configuration algorithm and test it in a dedicated flight test campaign where single servos are commanded to fixed pre-planned positions during flight to emulate the failure condition.

3.3.3. Altitude and Speed Control

Altitude rate and altitude control loops are cascaded around the integral load factor control of section 3.3.1.

$$\Delta nz_{cmd} = \frac{k_{i,\dot{h}}}{s}\left(k_{\dot{h}}(h_{cmd} - h) - \dot{h}\right) - k_{\dot{h}}\dot{h} - k_{\dot{h},V}V \quad (8)$$

A load factor increment Δnz_{turn} for turn compensation is added as a function of bank angle command. Altitude rate command is retained as a separate command input thereby providing a generic interface for either remote pilot inputs from a ground station or inputs created by trajectory generation algorithms.

A proportional-integral speed control loop offers a choice between a feedback of air speed measurement (V_a) and integral air speed error on thrust command (P_{cmd}) and ground speed measurement and integral ground speed error on thrust command.

$$P_{cmd} = \frac{k_{i,V}}{s}(V_{cmd} - V) - k_{V_a}V_a + k_{V,\dot{h}}\dot{h} \quad (9)$$

The resulting speed command interface complements the direct throttle command interface and can be used directly for remote pilot inputs from a ground control station. The ground speed command interface can in addition be used for inputs generated by 4-D trajectory generation algorithms.

3.3.4. Direction Control

The bank angle command system of section 3.3.1. is made directly available as interface for remote pilot inputs from the RPS (see FIG 14 for a flight test example turn). It can also be used as an interface for trajectory generation algorithms, mainly for mission purposes.

Traditional autopilot functions such as course acquire and hold functions are implemented in addition. For way-point-following, feedback cascades for track angle and cross-track error are provided. This functionality was originally designed for reduced flight technical error in lateral position in the context of conventional landing approaches [4] and has been re-used for Quadcruiser, offering improved mission performance when flying waypoint patterns.

3.4. Cruise Flight Test Results

Cruise flight has been flight tested in a limited test area leaving sufficient room for testing direction control options and altitude control but limiting the possibilities for straight and level flight or sustained climb/dive manoeuvres. Therefore further tests are planned in a larger test area.

An example flight path for a short flight comprising automatic take-off and hover flight to a suitable transition start position with aircraft pointing into the wind (red), transition from hover to cruise (green), cruise flight at constant altitude with course or bank commands selected by the pilot on the RPS (blue), transition back to hover (green), hover flight to the landing position and automatic landing (red) is shown in FIG 13. Transition acceleration requires a distance of approx. 200m and transition deceleration of approx. 300m in the presence of 10kts headwind.

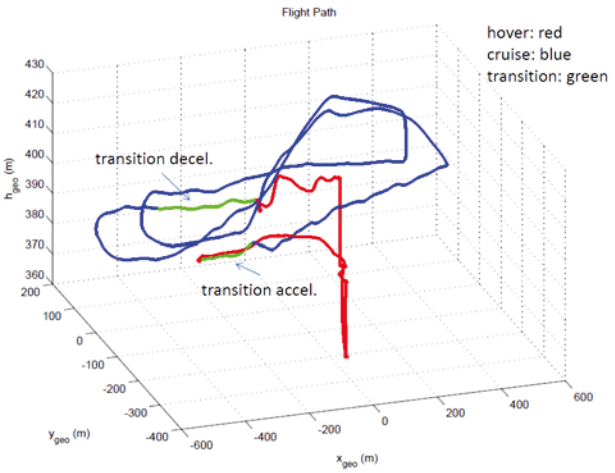

FIG 13. 3-d Flight Path of example flight

FIG 14 illustrates bank angle change manoeuvres when following waypoints and an altitude change manoeuvre commanded by the pilot on the RPS. Bank angle commands up to 35deg are shown. This leaves sufficient margin to the bank angle authority of 50deg for compensating wind.

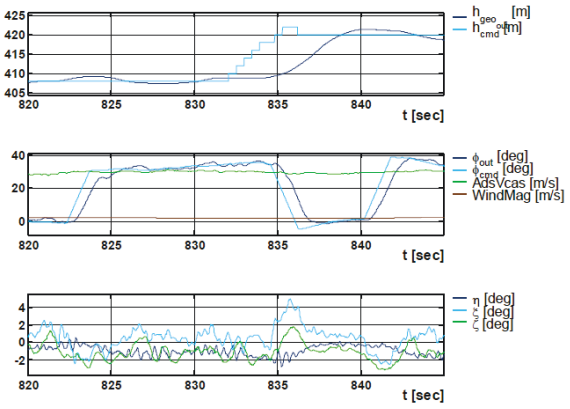

FIG 14. Altitude and bank angle change in cruise flight

A turn at 45deg bank at the low speed limit V_{minFCS} is shown in FIG 15. When the speed drops below the limit due to gusts the bank angle authority is reduced (supporting the stall protection functionality). At time 1395 the pilot increases the speed command to 30m/s and the autothrottle moves the PLA command to full thrust. The electric push motor follows with a small delay and the speed increases.

For flying speeds exceeding 35m/s (70kts) CAS in the turn, the chosen push propeller/pusher motor combination is not generating enough thrust.

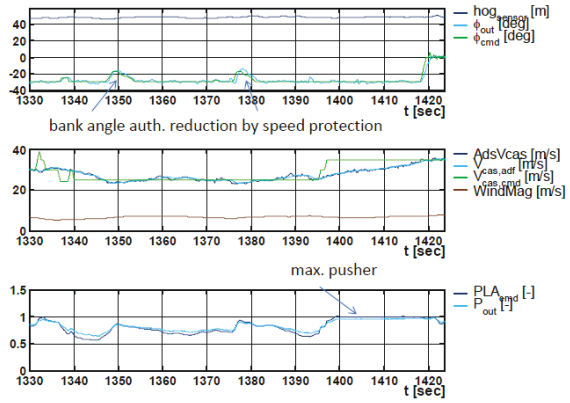

FIG 15. Low speed turn and acceleration in cruise flight

4. TRANSITION BETWEEN HOVER AND CRUISE FLIGHT

Originally plans were made to fly the subscale Quadcruiser in steady flight at all speeds between zero and the stall speed. For fear of losing attitudes and inertial speed measurements from the INS due to the high level of vibrations encountered when flying in “copter” mode (i.e. with the lift propellers generating most of the lift while being subject to radial flow conditions) it was decided to limit the exposure of the vehicle to the “copter” conditions to short transitions. Consequently, the transition from hover to cruise was set up as an acceleration manoeuvre with pusher motor at full power and the transition from cruise to hover as a deceleration manoeuvre with the push propeller switched off. This set-up was retained when it was later found that the “copter” mode was unattractive operationally due to the high power consumption.

4.1. Investigation of Flight Mechanic Characteristics by Flight Test (RC Control)

As steady state “copter” flight was not available for aerodynamic investigations, a sequence of transient manoeuvres was designed for the exploration of the “copter” flight conditions in a controlled manner.

At the beginning of the manoeuvres, the air vehicle was stabilised in hover at zero speed, then the push propeller was switched on and the aircraft was accelerated to a target speed with the pusher being switched off when the target speed was reached and the vehicle subsequently decelerated again. The blending in and out of the hover control system was done initially by the remote pilot using a conventional RC command unit, see e.g. FIG 17.

This approach allowed to expand the speed envelope of the subscale Quadcruiser in a safe manner and to identify the aerodynamic characteristics linked to the interferences between lift propellers, wing and empennage. During acceleration, two effects were identified which were more significant than expected. The first effect is a pitch-up

moment experienced when switching on the push propeller at zero speed (see FIG 16). This effect is attributed to an interference between push propeller downwash and the empennage. The second effect is a pitch-up experienced with increasing forward speed and still high lift contribution from the lift propellers (see FIG 16).

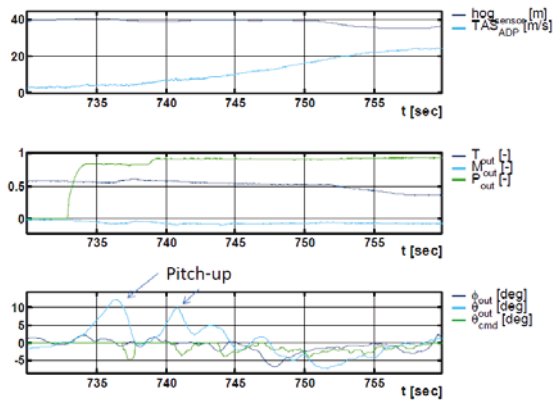

FIG 16. Pitch-up on pusher start-up for transition

This effect is attributed to an interference between the downwash of the wing and the aft lift propellers. In this situation the forward lift propellers are subject to radial flow conditions which increase lift (and drag) whereas the aft lift propellers see significantly less radial flow and consequently generated less lift. The second effect implies that high lift devices on the trailing edge of the wing (i.e. flaps and aileron) may not be beneficial for the transition between hover and cruise in contradiction to the original assumption that the increased aerodynamic lift would reduce the required lift propeller power and the associated vibrations. It is planned to investigate this issue in later flight tests with different flap & symmetric aileron schedules during the transition.

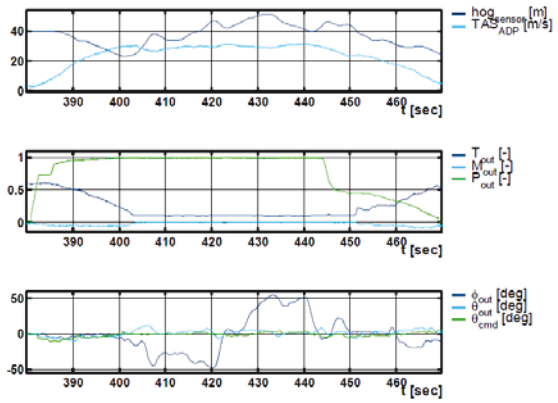

FIG 17. „Manual“ transition from hover to cruise

The pitch-up tendency could be compensated easily by the pilot (see θ_{cmd} in FIG 17). Based on the flight test results obtained, the flight mechanic model was updated and subsequently control laws were designed to address the flight mechanic characteristics of the air vehicle. In addition, a more detailed aerodynamic investigation using Navier-Stokes CFD analysis was triggered.

The return-transition from cruise to hover did not reveal unexpected aerodynamic effects.

4.2. Wind Measurement and Estimation

During cruise flight, wind conditions are estimated from a comparison of inertial speeds (measured by the IMU) and air speed components (estimated from dynamic pressure and angle of attack measurements) in geodetic axes. The dynamic pressure measurement is available down to roughly 10kts (5m/s) forward airspeed. Therefore the same approach cannot be used in Hover flight and in particular when the vehicle is subject to tailwind conditions. For Hover flight, a wind estimate (with north and east components $\hat{v}_{w,N}, \hat{v}_{w,E}$) is provided from inertial speed measurements and inertial pitch and roll attitude measurements by means of an observer using a model of the horizontal accelerations caused by tilting the lift propellers around the pitch and roll axes respectively ($g \sin\theta, g \sin\varphi$) and the approximated drag forces acting on the vehicle ($-C_x/m\,\hat{v}_{a,x}, -C_y/m\,\hat{v}_{a,y}$). The observer is limited to the speed components in the horizontal plane and takes the form

$$\dot{\hat{x}} = A\hat{x} + Bu - L(C\hat{x} - y) \tag{10}$$

with (projected) air speed components $\hat{v}_{a,x}, \hat{v}_{a,y}$ along body x and y axes and wind speed components in geodetic (north, east) axes $\hat{v}_{w,N}, \hat{v}_{w,E}$ chosen as observer states $\hat{x}$. Heading measurement is available for transformation between geodetic and body axes and inertial speed measurements $v_{k,i\,(INS)}$ constitute the measurement vector y, i.e.

$$\begin{aligned}
\dot{\hat{v}}_{a,x} &= -C_x/m\,\hat{v}_{a,x} - g\sin\theta - l_x\left(\hat{v}_{k,x} - v_{k,x(INS)}\right)\\
\dot{\hat{v}}_{a,y} &= -C_y/m\,\hat{v}_{a,y} + g\sin\varphi - l_x\left(\hat{v}_{k,y} - v_{k,y(INS)}\right)\\
\dot{\hat{v}}_{w,N} &= -l_N\left(\hat{v}_{k,N} - v_{k,N(INS)}\right)\\
\dot{\hat{v}}_{w,E} &= -l_E\left(\hat{v}_{k,E} - v_{k,E(INS)}\right)
\end{aligned} \tag{11}$$

and $\hat{v}_{k,N} = \hat{v}_{a,N} - \hat{v}_{w,N}$ $\hat{v}_{k,E} = \hat{v}_{a,E} - \hat{v}_{w,E}$, where l_i denotes the observer gains. The estimated wind conditions are displayed to the pilot on the RPS and the airspeed estimate is used for blending of hover and cruise control laws during transitions.

5. AUTOMATIC TRANSITION

After flight testing the basic control laws for hover and cruise, autopilot functions for automatic transition were added to the flight control system. Automatic transitions are currently only performed on straight legs. Therefore they are limited to headwind conditions as this minimizes the distance required.

5.1. Set-Up and Implementation of the Control Laws for Transition

During transition between hover and cruise flight both the lift control system and the cruise control system are active in parallel. The combination of the two systems is organised using speed-dependent blending functions.

The integral command systems for the roll and pitch axis are coupled in the blend-over region ($V_{maxHover} < V < VS0$). In the yaw axis, a yaw damper is realised via lift propellers and rudder leaving it to the strong weather-cock stability properties of the Quadcruiser configuration to ensure small angles-of-sideslip.

The feedbacks for stability augmentation and attitude control of the two systems are blended in and out as a function of speed and integrators are changed to first-

order lags. Consequently, all control surfaces return to a scheduled position for speeds inside the hover flight envelope and the lift propellers are all running at idle speed for speeds beyond the stall speed of the air vehicle. Lift propellers are further switched off when the minimum cruise speed V_{minFCS} with

(12) $V_{minFCS} = 1.2 * VS0$

is exceeded, where VS0 denotes the Stall speed.

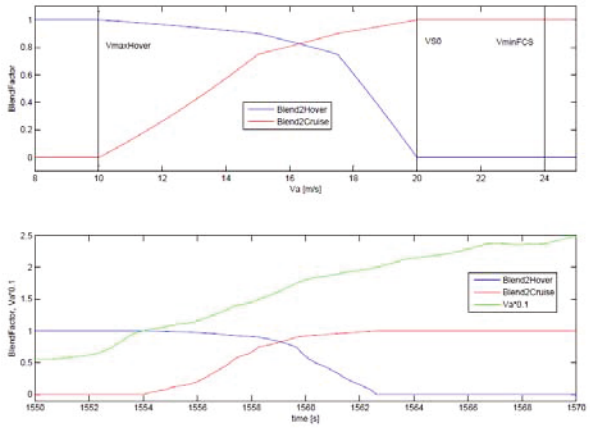

FIG 18. Blending between hover and cruise

5.2. Transition from Hover to Cruise

The autopilot for automatic transition consists of an altitude rate and altitude control loop in the vertical axis and a bank angle hold loop in the roll axis. Moding elements are added for activation of the transition from a remote pilot station (RPS).

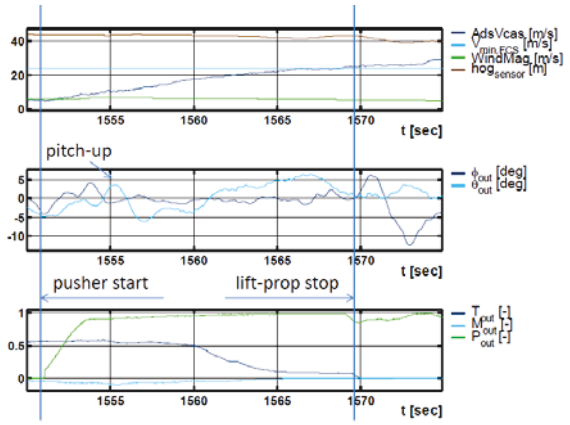

FIG 19. “Automatic” transition acceleration

To avoid and compensate the initial pitch-up experienced when switching on the push propeller, the hover control system is activated in addition for acceleration at low speeds. Consequently, the aircraft is commanded to pitch down resulting in a forward tilt of the lift vector from the lift propellers. This pitch down command is blended out with speed, so that a zero pitch attitude is expected when the aircraft accelerates beyond the maximum hover speed $V_{maxHover}$. From this point, the hover system is blended out. With decreasing speed of the lift propellers the associated drag reduces and forward acceleration of the vehicle increases. Pitch attitude is kept at around zero through this “copter” phase to avoid creating a “backward pulling” lift component from the hover system. For generating lift on the wing an angle-of-attack of approx. 5deg has been found preferable. Ideally this would be generated by a small dive angle of 5deg, resulting in a fast acceleration accompanied by a small altitude loss. During initial flight tests however (see time histories in FIG 19) the pitch attitude remained positive so that no altitude loss occured. Once V_{minFCS} is reached, the lift propellers are switched off and only the cruise control laws remain active.

Flight tests were conducted in the presence of benign wind conditions with e.g. 5m/s (10kts) headwind in the example case of FIG 19.

5.3. Transition from Cruise to Hover

The return transition is characterised by three phases caused by Control Law moding. In the first phase, the push motor is switched off (the propeller is wind-milling) and the vehicle decelerates in level flight. In the second phase, when speed reduces below V_{minFCS} the lift motors are started up. As the collective lift is increased, the aircraft pitches up. Consequently the lift system contributes to the deceleration of the vehicle. For $V < V_{maxHover}$ (i.e. the vehicle enters the hover flight envelope) the third phase starts where the hover laws control flight path and speed and the cruise control laws are faded out. At zero inertial speed, the hover control laws command the pitch attitude required to compensate the wind.

The return transition is illustrated by flight test results shown in FIG 20. Altitude remains tightly controlled within a 3m band during the manoeuvre. The manoeuvre is performed into headwind (5m/s; 10kts) conditions and takes roughly 15sec. and a distance of 270m for coming to a full stop from a start speed of 30m/s (calibrated) air speed (25m/s ground speed).

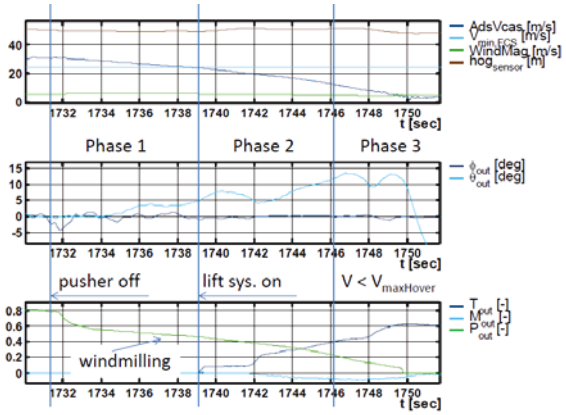

FIG 20. “Automated” transition deceleration

Clearly, from an operational perspective it is important to ensure that the position reached at the end of the transition can be accurately predicted (without flying long distances in hover mode). In addition, the energy consumption during the transition phases should be reduced to a minimum as battery size and weight are driving the Quadcruiser air vehicle configuration. Therefore, further optimisation is planned with respect to the automatic transition control laws.

6. AUTOMATIC VTOL

Automatic vertical take-off and landing (VTOL) is implemented based on the control laws for hover flight (see section 3). As wing and empennage make the Quadcruiser configuration more sensitive to gusts and

turbulence than conventional quattro- or octocopters, disturbance rejection is the biggest challenge for automatic VTOL.

6.1. Automatic Take-Off

In preparation for take-off, the current position and attitudes of the vehicle are stored so that a height-over-ground (*hog*) signal relative to the take-off position based on GPS and inertial data can be made available for control law moding. A weight-on-wheel signal is not required. For take-off in the presence of stronger wind (i.e. exceeding 10kts) the vehicle is turned into the wind before take-off.

The control laws for automatic take-off are designed so that

1) ground contact by propellers or wing tips is avoided;
2) containment of the vehicle in a small area around the take-off position is ensured in the presence of wind;
3) the vehicle is stabilised in headwind condition for transition into cruise flight.

The first issue is addressed by a fast ramp up of the lift motors in the initial take-off phase, from idle thrust to a lift value of more than 110% of weight so that the vehicle moves rapidly out of ground vicinity, reducing its sensitivity to disturbance moments from gusts and turbulence. In this first phase and up to an altitude of 1.5m *hog*, a heave motion perpendicular to the start surface is commanded and only proportional feedbacks are active so that integrator wind-up is avoided while the aircraft is still on ground. As the aircraft takes off, disturbance moments are countered by the control system but the aircraft drifts slightly in the direction of the wind until the wind forces are balanced.

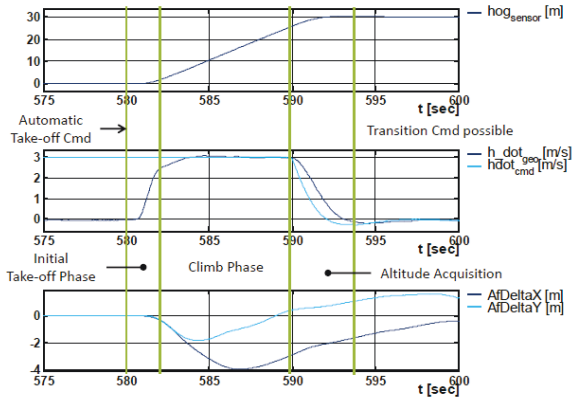

FIG 21. Automatic Take-Off

In the subsequent climb phase, issue 2) is addressed by activating the (integral) hover control laws of section 3 with position controlled to the lateral and horizontal take-off position and a constant altitude rate commanded in the vertical axis. Finally, an altitude acquisition loop is closed, commanding the aircraft to a position 30m above the take-off position with the aircraft pointing into the wind. This addresses issue 3) and makes it possible to directly continue with a transition into cruise flight.

The automatic take-off is illustrated by flight test results shown in FIG 21. After the automatic take-off command the fast ramp up of the lift motors generates a fast increase of the altitude rate during the initial take-off phase which lasts 2s in the example case. The take-off was performed in headwind condition (3m/s). Consequently a position deviation is visible with a maximum (of 4m) in the climb phase at 15m hog. At this point the wind forces were balanced and the position deviation was reduced after that. The take-off position was reached after the automatic take-off was finished.

6.2. Automatic Landing

Automatic landing is divided in two phases named approach and touch-down respectively. A radar altitude sensor provides a height-over-ground information which is used for switching from the first to the latter at a trigger altitude of 4m hog.

The design aims for automatic landing are

- avoiding ground contact by propellers or wing tips;
- touch-down at the landing position selected by the pilot;

During the approach phase, the hover control laws of section 3 are activated, with position controlled to the landing point selected by the pilot and a constant altitude rate commanded in the vertical axis.

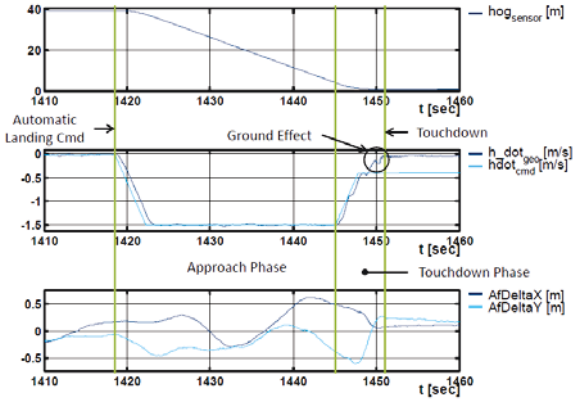

FIG 22. Automatic Landing with wind smaller than 5kts

In the touch-down phase, the sink rate command is reduced. Directly above the surface, the sink rate is further reduced by the ground effect so that the vehicle touches down gently.

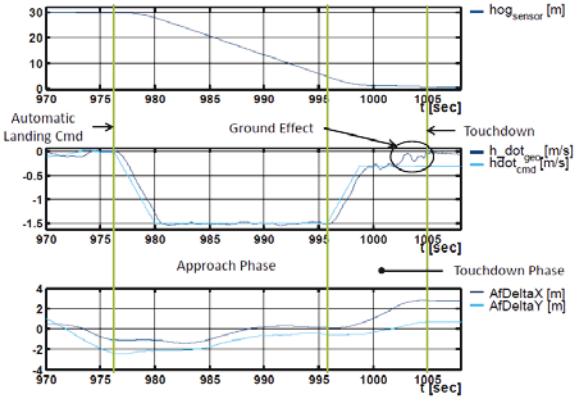

FIG 23. Automatic Landing with wind larger than 5kts

For landings performed in the presence of (more than 5kts of) wind a drift of the aircraft away from the commanded landing position was observed in flight test during the touch-down phase. The forces causing the drift were attributed to the ground effect, wind and turbulence. It was

concluded that the sink rate had to be reduced in the presence of wind to give the position control loop more time to re-adjust to changing wind speeds close to the ground.

Consequently, the trigger altitude and the sink rate command of the touch-down phase are made a function of the wind estimate (provided by the observer of section 4.2) calculated and stored at the start of the automatic landing.

After touch-down, the integral heave control loop rapidly reduces the collective lift.

Automatic landing flight test results for two different wind conditions are shown in FIG 22 and FIG 23. In both example cases the ground effect reduced the altitude rate directly before touch-down which ensures that the Quadcruiser touches down gently. In the presence of light wind (3.5kts) (see FIG 22) no position deviation is visible after touch-down. For the example case with wind larger than 5kts (see FIG 23) the trigger altitude was higher (5m) and the commanded altitude rate smaller (0.3m/s instead of 0.4m/s) to ensure that the position loop has more time for readjustment. Still a position deviation of 3m was observed.

7. CONCLUSION

Flight Control Laws for the hybrid Quadcruiser remotely piloted air vehicle have been developed. Flight Control Laws were developed separately for the conventional cruise flight configuration and for the Quadcopter-like hover configuration. For transitions between hover and cruise, both flight control laws are active. During transition the feedbacks of the two control laws are blended in and out as a function of speed. Control law prototypes have been implemented and flight-test-demonstrated on a subscale Quadcruiser experimental vehicle. Automatic control of hover and cruise was demonstrated first, automatic transition and automatic vertical take-off and landing next.

From a scientific point of view, the use of the subscale experimental vehicle has turned out to be advantageous for early identification of closed-loop effects such as vibration propagation and the environmental effects such as the ground effect during landing. For pure identification of aerodynamics however, wind tunnel tests would probably be more efficient.

From a project point of view, the subscale experimental offers a chance to present the unconventional Quadcruiser configuration to potential customers in flight test demonstrations and to support trade-offs for system design decisions such as defining the service speed envelope of hover flight.

The flight test results show that the prototype control laws can handle the failure-free air vehicle in the presence of considerable environmental disturbances. As the Quadcruiser project aims at civil certification of the RPA for operation over populated areas, the focus of the development is now shifted to system failure handling and the further enhancement of envelope protection functions in order to address certification requirements such as those of CS-LURS [5] and CS-LUAS [6]. Minimisation of the required excess thrust in hover and optimisation of the transition between hover and cruise are additional topics for further control law development.

References

[1] R. Brockhaus, W. Alles, R. Luckner; *„Flugregelung“*; 3. Auflage, 2011; Springer Verlag, Berlin Heidelberg, ISBN 978-3-642-01442-0
[2] M. Haimerl, „*Development of a Flight Control Algorithm for the VTOL unmanned Aerial Vehicle Quadcruiser*“, M.S. thesis, 2015
[3] M. Haimerl, F. Binz, S. Engels, D. Moormann, *“Entwicklung einer modifizierten, instationären Wirbelgittermethode für eine senkrechtstartfähige Flugzeugkonfiguration”*, DLRK, 2017
[4] J. van Tooren, R. Hammon; *„Experiences with the Barracuda UAV Auto Flight System“;* EuroGNC 2013, Delft.
[5] JARUS CS-LURS; *“Certification Specifications for Light Unmanned Rotorcraft Systems”*; V1.0;30.10.2013
[6] JARUS CS-LUAS; *“Recommendations for Certification of Light Unmanned Aeroplane Systems”*; Ed. 0.3, Nov. 2016

Acknowledgements

This article contains results of the Lufo V-2 collaborative research projet “SiFliegeR”, co-funded by the German Federal Ministry of Economic Affairs and Energy.

Gefördert durch:

Bundesministerium für Wirtschaft und Energie

aufgrund eines Beschlusses des Deutschen Bundestages